First-principles prediction of stable SiC cage structures and their synthesis pathways

Pascal Pochet,[1,*] Luigi Genovese,[2,†] Damien Caliste,[1] Ian Rousseau,[1] Stefan Goedecker,[3] and Thierry Deutsch[1]
[1]*Laboratoire de Simulation Atomistique (L_Sim), SP2M, INAC, CEA-UJF, 17 Av. des Martyrs, 38054 Grenoble, France*
[2]*European Synchrotron Radiation Facility, 6 rue Horowitz, BP 220, 38043 Grenoble, France*
[3]*Institut für Physik, Universität Basel, Klingelbergstr. 82, 4056 Basel, Switzerland*
(Received 3 March 2010; revised manuscript received 15 June 2010; published 21 July 2010)

In this paper we use density functional theory calculations to investigate the structure and the stability of different SiC cagelike clusters. In addition to the fullerene family and the mixed four and six membered ring family, we introduce a family based on reconstructed nanotube slices. We propose an alternative synthesis pathway starting from SiC nanotubes.

DOI: 10.1103/PhysRevB.82.035431 PACS number(s): 61.48.−c, 61.46.Bc, 71.15.Mb

Carbon-based nanostructures exhibit many different low-dimensional allotropes (fullerenes, nanotubes, etc.). This leads to a wide spectrum of possible physical properties. Adding silicon atoms to such structures is therefore of great interest, both from a theoretical and applied point of view. While it has been recently pointed out[1] that such SiC nanostructures will be well-suited for applications in various important fields such as micro- electronics and catalysis, their possible synthesis is still an issue: only SiC nanotubes have been obtained[2] and the tentative synthesis of SiC fullerenes via the substitution of C atoms by Si atoms in carbon fullerenes has failed (see, e.g., Ref. 3). In this paper we use density functional theory (DFT) calculations to investigate the structure and the stability of different stoichiometric SiC cagelike clusters. We propose an alternative synthesis pathway starting from SiC nanotubes.

The DFT calculations are performed with the BigDFT code,[4] which uses a systematic wavelet basis set. The number of basis functions is chosen in such a way that our energy results per Si-C pair are accurate within 1 meV. Geometries are considered optimized when the forces between two atoms are less than 2 meV/Å. The exchange-correlation functional used for the calculation is the PBE approximation,[5] and the pseudopotentials used are of the HGH form,[6] in the Krack variant.[7] Isolated boundary conditions are used both for the Kohn-Sham electronic orbitals and the calculation of the electrostatic Hartree potential.[8] Hence no supercell approximation is needed. The stability of a given SiC cluster is classified in terms of the energy per SiC pair. All the structures we analyzed have SiC sp^2-like bonds. For this reason, we choose as a reference energy the energy per SiC pair of a single SiC sheet. This is calculated with the BigDFT code with explicit surface boundary conditions, which are again consistently used both for the Kohn-Sham electronic orbitals and the calculation of the electrostatic Hartree potential.[9]

In the recent years several theoretical studies have been made on the stability of different cagelike clusters of SiC. In the absence of experimentally characterized objects, both the cage structure and the local chemical arrangement were investigated. Most of these studies were modeled on the basis of carbon fullerene cages (FC). Matsubara and Massobrio[10] have studied the stability of $C_{60-p}Si_p$ heterofullerenes, in a chemical arrangement which separates Si and C regions on the cage surface. Other analyses of cages with this separated Si/C local ordering have been carried out by Ray's group.[11,12] For a FC based structure, the Si/C separation is imposed by the presence of pentagons in the original FC, that forbids the realization of a fully alternating Si-C conformation (each Si having three C neighbors, and vice versa). Moreover, a study of the dynamical stability of such cages[13] has shown that such cages tend to fragment due to the unstable character of the Si part of the cage. At the same time, several calculations[14–16] have shown that the alternating conformation is the preferred for SiC nanotubes. Other studies[17] have been carried out by taking into account cagelike structures without pentagons composed only of squares and hexagons (4–6 cages). Such structures have six rhombi on their surface, and they are more or less deformed depending on the relative position of the squares. Their conformation have been originally pointed out in the case of BN clusters,[18] and a theoretical study of these compounds have revealed that they are good candidates for high-stability stoichiometric cages. Cage-like clusters of this shape have already been analyzed for other materials (see, e.g., Refs. 17 and 19–21), showing a high stability with respect to other shapes. When these squares are placed in a way that gives an octahedral symmetry we obtain nano-octahedral structures which have been shown to exist in several layered compounds.[19] Such structural arrangement permits the alternating Si-C conformation which, from the above mentioned nanotubes studies, appears to be preferred for SiC sp^2 bonding.

We start our analysis by considering SiC cages which have same number of atoms as the carbon FC. Our study focuses on stoichiometric compounds (Si to C ratio of 1:1), with fully alternating chemical ordering. Our choice to analyze fully alternating cages is motivated by two reasons. First of all, from the above mentioned study,[13] it is unlikely that a dynamically stable stoichiometric cage will present a fully segregated conformation. We prefer to focus on conformations in which the $sp2$ character of the bonding is preserved. Second, we have also analyzed the possibility of partial Si-C segregation, namely nonfully alternating ordering. Our results have shown (see below) that these conformations are energetically defavorable with respect to the Si-C-Si conformation. In addition, the predicted chemical ordering for SiC nanotubes seems to be fully alternating. We will see in the following that this fact will be of interest to explore synthesis pathways of these cages.

In Fig. 1, we show different structures we have considered with 30 SiC couples. All these structures are local minima in

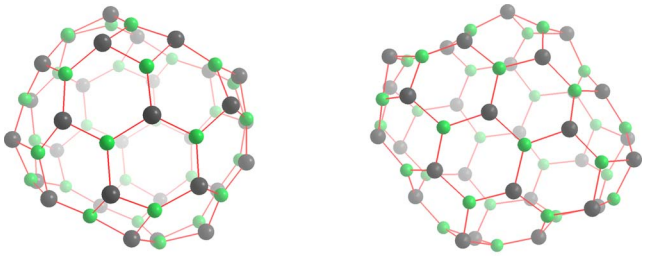

(a) 90 bonds, 719 meV (b) 90 bonds, 679 meV

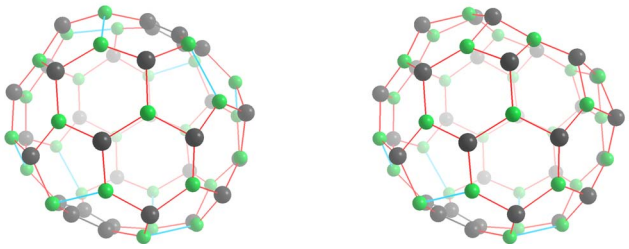

(c) 70 bonds, 744 meV (d) 80 bonds, 736 meV

FIG. 1. (Color online) Dependence of the energetic stability from the chemical ordering. Different stoichiometric structures of SiC cages of 60 atoms. The number of alternating Si(green)-C(black) bonds and the energy per SiC pair (meV) are indicated. A partially segregated chemical ordering is energetically defavorable wrt a fully alternating one.

configuration space. In panel (a) and (b) we show structures which have 90 Si-C $sp2$-like bondings, which means that they are fully alternated. The energy per SiC couple is indicated, measured with respect to the reference of the SiC planar monolayer. In panel (c) and (d) we have presented two examples of nonfully alternating structures, which show a partial aggregation of carbon atoms in pentagonal structures. The cage (c) is a Si-doped FC. Both structures are more energetic that the ones with 90 bondings. Other configurations which are nonfully alternating exhibit similar behavior: partial Si-C segregation always tends to increase the energy of the cage. This fact shows that the fully alternating sector of the configuration space has tendency to preserve the Si-C-Si conformation rather that to favor Si or C aggregation on the cage surface.

We now concentrate our analysis cages 1(a) and 1(b). We will see that these objects are actually representatives of wider families of nanoscaled SiC cages. The cage of Fig. 1(a) has a somewhat cylindrical shape, with two "holes" at the terminations. Such structures can be obtained from n "slices" of an (m,m) armchair-type nanotube, by recombining the dangling bonds at the terminations. This creates a double-terminated single-walled SiC nanotube slice (NTSn). The termination contains m squares and one almost flat $2m$ polygon on each side of the NTS (e.g., a decagon for the cage in Fig. 1(a), which is the NTS6 with $m=5$). In the bottom panel of Fig. 2 we have drawn the termination of bigger NTSn($n \geq 12$) cages of diameter $m=6,8,10$. This NTS termination is realized by deforming the original nanotube shape. These terminations are basically caps of the finite tubes formed by reorganization of the dangling bonds. In semi-infinite nanotubes, such behavior is also seen in other elements such as BN (Refs. 22 and 23) or AlN.[24] In these studies it has been pointed out that for the considered diameters, in the case of AlN such caps are formed simply when the open finite tube are optimized, whereas on BN a barrier prevents a rearrangement from a configuration in which the dangling bonds form a 2×1-like reconstruction at the tube end. This undeformed 2×1-like termination can be built also in the SiC case from the raw cut as illustrated on the right panel of Fig. 2. Due to the remaining Si-C dangling bonds, for the cage of Fig. 1(a) such a termination is less stable than the NTS termination where all the dangling bonds are recombined. However, as we will explain in the following, we may determine a threshold diameter (m_0) of the cage. The NTS termination will be unstable for diameters bigger that this threshold.

We have considered NTSn families with $n=6,8,12,18,24$ with different values of m. Each of these cages is a local minimum in the configuration space of $2nm$ atoms. The energies per SiC pair of the relaxed geometries are plotted in Fig. 2. For each series of a given number of slices n there is an optimal configuration which has the minimum value of energy per pair. The value of such optimal diameter m^* increases with the length n of the cage family. Moreover, for a given diameter the configuration with highest number of slices has always a lower value of energy per SiC pair. This means that, for any of the cages we have considered, two NTS structures with the same diameter are potentially very reactive since they would prefer to arrange in a bigger NTS cage.

Thanks to these observations, we can draw several conclusions on the geometry of these structures. As the diameter m of the cage increases, the curvature of the central part of the cage decreases as $[\mathcal{O}(1/m)]$, and its local ordering tends to be more similar to the single SiC sheet, which is lower in energy. This would favor cages of high diameters. For the NTS cages, this mechanism is in competition with the deformation of the termination, which is more and more important, and energetically more costly as the diameter of the cage increases. Such terminations have stretched/compressed bonds and spherical form [curvature of $\mathcal{O}(\sqrt{m})$]. The optimal diameter is reached when the stabilization energy induced by the decrease of the curvature in the body balances the deformation energy generated in the termination. Moreover, at a given diameter m_0 the termination with a $2m_0$ polygon is less favorable than a 2×1-like termination, whose energetic contribution is dominated by the stretching induced by the bond reconstruction. For $m>m_0$, we have thus found at least one atomic arrangement of the termination which is lower in energy than the corresponding NTS. For creating NTS-type SiC cages, one has thus to start from nanotubes with diameters which are smaller than m_0.

To give a quantitative description of these considerations, we can write the energy of a NTSn cage as the sum of the energy of a slice in the internal part of the structure and the energy associated with a deformed termination. The expressions for these contributions can be obtained from the isotropic shell model of elasticity theory, as has already been done for monolayers of materials with hexagonal symmetry in 2d lattices (see, e.g., Refs. 25 and 26). Essentially, we found that

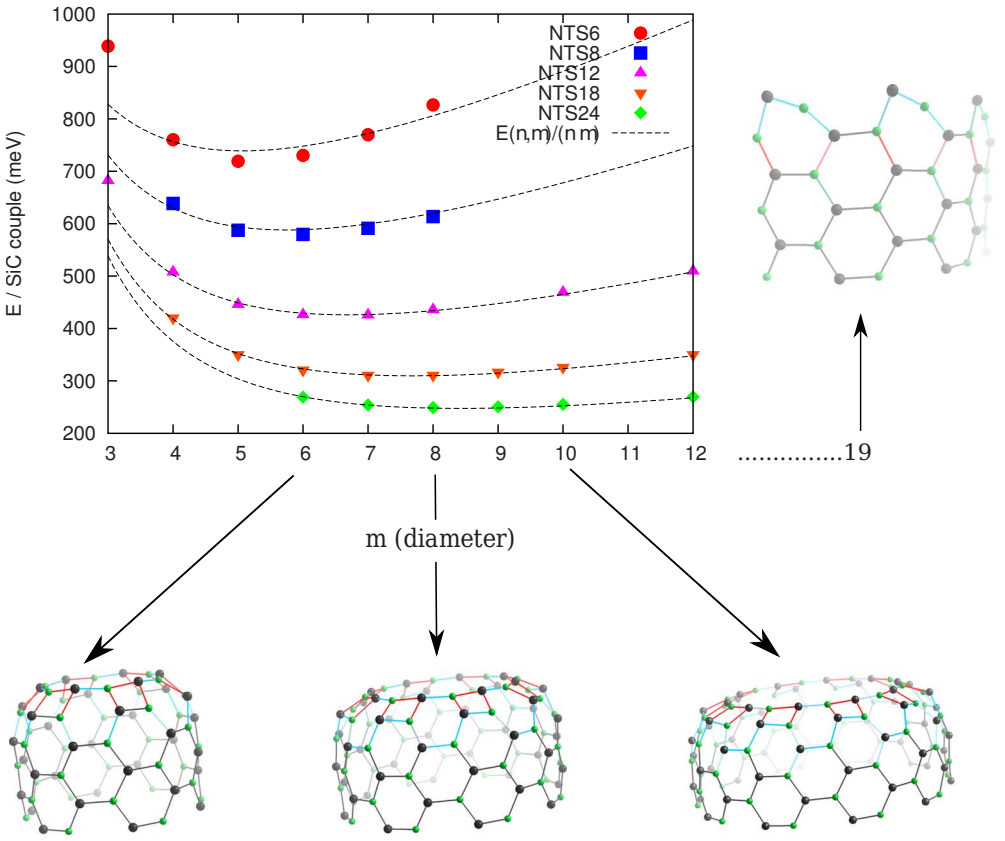

FIG. 2. (Color online) Energetic behavior of SiC NTSn families. Energy per Si-C pair of different NTSn cages as a function of their diameter m. Each cage has nm Si-C pairs. The dotted line indicates the results from the model described in the Appendix. The correct optimal diameter for each family is reproduced as a result of the balance between the energy of the body $[\mathcal{O}(1/m)]$ and of the termination of the cage $[\mathcal{O}(\sqrt{m})]$. The structure and terminations of the NTS SiC cages are drawn for $m=6,8,10$ diameters on the bottom panel. Such terminations have stretched (red/dark gray) and compressed (blue/light gray) bonds. The termination appears more deformed as the diameter m increases. An illustration of the 2×1-like termination is drawn on the right panel. The latter termination is predicted to be more stable for bigger diameter $(m\geq19)$.

the energetic behavior (see the Appendix) is primarily driven by the square of the curvature (flexural rigidity), corrected by terms which take into account stretching and compression (Poisson ratio). These simple expressions provide us with a simple energetic model (see the Appendix), whose results are plotted in Fig. 2, in agreement with DFT calculations. In particular, the correct optimal diameter m^* for each family is reproduced, which confirms our physical interpretation for the existence of a minimum. Also the energy cost of a termination can be studied as a function of m with this model. As already pointed out, for low diameters, the 2×1-like terminations are only metastable states and the polygonal termination will be preferred while NTSn cages of higher diameter will prefer a 2×1 reconstruction. The above model gives an estimation of this critical radius of $m_0=19$. We stress that the determination of m_0 presented here is based on considering only the 2×1-like termination as an alternative to the NTS one. Other kind of arrangements may be more favorable than the 2×1 case for diameters around m_0. The important point here is that, whatever the actual picture is, the polygonal termination of the NTS cages will not be stable for high diameters. Also, the tendency of two cages NTSn_1 and NTSn_2 to "fuse" in one longer NTS(n_1+n_2) cage is predicted by this model, with a energy gain which only depends of the diameter.

Therefore, given a fully alternating chemical ordering, a SiC cage tends to prefer a structural arrangement which minimizes the local deformations with respect to the plain SiC monolayer, in particular by minimizing its curvature, which is easier for cagelike shapes. The reasons why this occurs can be generalized to different $sp2$-like compounds, explaining the different behavior of the termination depending of the material.

As a parameter of stability, we have also calculated the HOMO-LUMO gap of the NTS cages. Results are indicated in Fig. 3. The value of the gap are distributed around a value of 2.1 eV, and are relatively constant as a function of the diameter of the cages. It can be seen that, for each family except the NTS6 cages, the value of the gap tends to decrease for cages which have diameter bigger than the optimal diameter m^*. The NTS cages which have big diameter are thus more reactive chemically. The NTS6 family slightly deviates from these trends $[m^*(6)=5]$. The reason for this is probably related to the relatively little number of slices. The deformation induced by the termination is present throughout the whole cage, and this makes the cages more reactive.

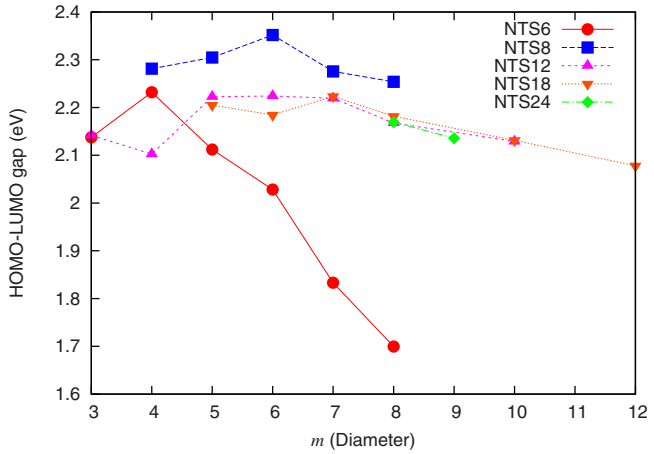

FIG. 3. (Color online) HOMO-LUMO gaps of some cages belonging to the NTS*n* families, as a function of their diameter *m*.

In addition to the NTS*n* cages, we have considered the family to which the cage 1(b) belongs. This is the set of 4–6 cages which have only squares and hexagons on the cage surface. A case of particular interest is when the six squares are placed along an octahedral symmetry. We have considered octahedral structures of 4–6 SiC cages of 36, 48, 108, and 192 Si-C couples, and nonoctahedral cages of 18, 24, 30 couples. Results are plotted in Fig. 4, as a function of the number of SiC pairs. Such cages have a value of energy per pair lower than the most stable NTS*n* cage with the same number of atoms. In contrast to the NTS*n* families, the energy per SiC pair decreases continuously with increasing size. Since the cage surface is mostly made by hexagons, the average local structure of these cages is close to the undeformed SiC sheet, and is only altered by the presence of the 6 squares. As for the NTS family, the energetic behavior is primarily driven by the curvature of the cage.

Therefore, we have found that (at least for some sizes) the NTS*n* are not the preferred alternating conformation SiC cages, since there exist structures which are (on average) locally more similar to the plain SiC monolayer, which has pure, perfectly balanced, sp^2 SiC bonding. Nonetheless, this fact does not imply that NTS cages are not stable. Indeed, due to their topology, the 4–6 conformations cannot be generated by local modification of the NTS*n* cages, nanotubes, or SiC heterofullerenes. Only a global rearrangement of the atomic position may connect the 4–6 cage to any of the structures described above.

Our DFT analysis permits to draw several important conclusions on the synthesis pathways of SiC cages. As possible candidates to synthesis, two families of SiC cages have been considered, the NTS*n* and the 4–6 cages. The synthesis of a stable stoichiometric cage will most likely be impossible by substituting Si atoms on carbon FC. Indeed, at the beginning of the process Si atoms would tend to aggregate, and the recovering of the alternating bonding will become more and more difficult as the Si:C ratio of the cage increases. This is due to the fact that a spatially separated Si/C chemical ordering is energetically preferred at lower concentration.[10] At a critical Si concentration, the *sp*3-like Si-Si bondings will tend to destroy the cage structure. The existence of such critical behavior for dynamical properties of Si_pC_{60-p} heterofullerenes has been already pointed out,[13] in which a critical value of $p=20$ was predicted.

In contrast to problem associated to doped FC, NTS-type cages can be obtained directly in an alternating bonding by cutting a SiC nanotube in chunks. This can be done for example by using the established cutting techniques for carbon nanotubes (see, e.g., Ref. 27). The cut reconstruction, leading to the closing of the cage with two polygons, is found to be energetically defavorable for tube diameter bigger than 3.2 nm. For all of the cages analyzed in this study, which have diameters lower than 2 nm, this reconstruction occurs spontaneously. Nevertheless as a consequence of the curvature minimization, the NTS cages will always tend to unify into bigger cages, locally more similar to nanotubes. This tendency should be properly taken into account during synthesis

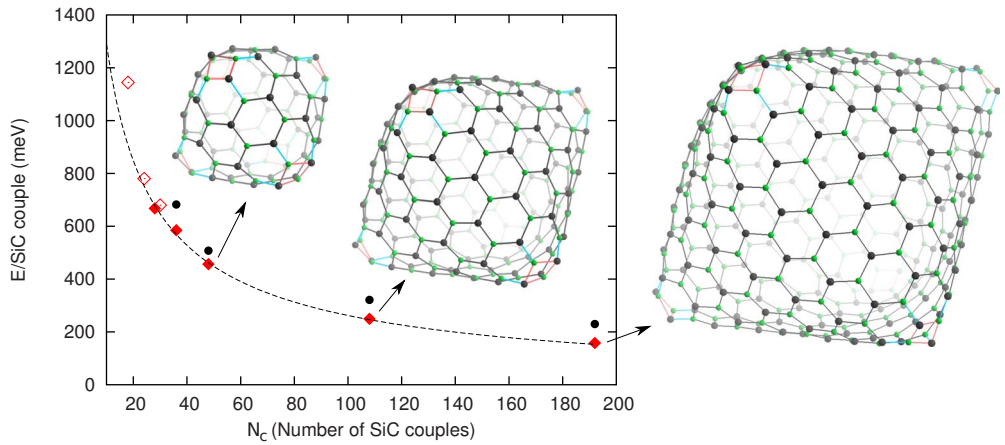

FIG. 4. (Color online) Energy per SiC pair of the 4–6 cages. We have considered octahedral structures of 4–6 SiC cages (filled diamonds) and nonoctahedral cages (empty diamonds). The main contribution to the energy of these structures comes from the spheroidal curvature as illustrated for the cages of size 96, 216, 384. This curvature decreases as the number of pair N_c increases $[\mathcal{O}(1/\sqrt{N_c})]$ (see the Appendix). These structures have also stretched (red/dark gray) and compressed (blue/light gray) bonds located around the squares whatever their size. The black dotted line indicates the result from the model fitted on cages with octahedral shape. The energies of the most stable NTS*n* cage (filled circles) for a given number of pairs is indicated.

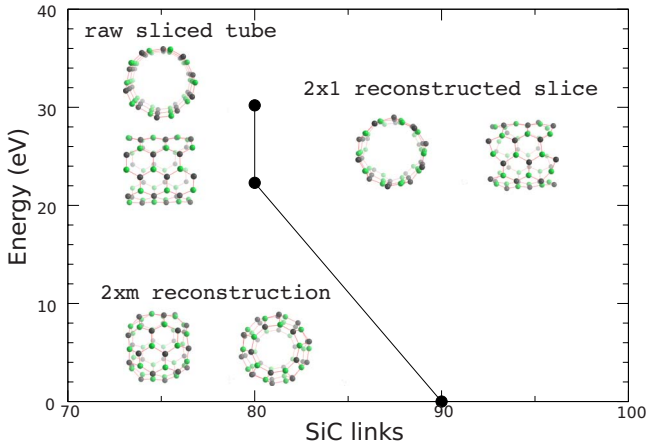

FIG. 5. (Color online) Different structures originated from the cut of $n=6$ slices of a (5,5) armchair nanotube (60 atoms). The dangling bonds of the unreconstructed cut can recombine in a 2×1-like reconstruction or into the NTSn structure, which is more stable since it has a bigger number of Si-C bondings, even tough is more deformed.

to avoid an immediate recombination of the NTSn cage with the original nanotube. Even though the NTS cages are not the global minimum for the considered cage size, their particular topology protects them from structural rearrangements which will lead to more stable structures such as the 4–6 cages. The synthesis of SiC 4–6 cages has not been achieved so far[17] and should according to our findings require high temperature processes. The NTS cages on the other hand could be synthesized by starting from existing intermediate SiC nanostructures. Our results thus help to explain the lack of experimental evidence in producing stoichiometric SiC cagelike clusters and stipulate under which conditions the experimental synthesis of these interesting nanoscale objects might be possible.

This work was performed using HPC resources from GENCI-CINES (Grant No. 009- c2009096194). Support from the Swiss National Science foundation and CSCS is also acknowledged.

APPENDIX: DESCRIPTION OF THE ENERGETIC MODEL FOR THE NTSn CAGES

The NTSn SiC cages can be seen as suitable rearrangements of the structure which results from cutting a SiC (m,m) armchair nanotube in chunks of n slices. As a consequence, a cage which belongs to an NTSn has properties which depend of the diameter of the original nanotube, which is linearly dependent of m.

We have analyzed the structures in terms of their geometry such as to find a relation between the structural arrangement and the energetic stability, in particular by taking into account the local deformation with respect to the undeformed SiC monolayer, which is lower in energy. In Fig. 5 the process of the creation of a NTS6 cage of diameter 5 is sketched. The dangling bonds of the original nanotube tend to recombine, first in a 2×1-like reconstruction, then by deforming the structure such as to obtain the NTS termination.

This deformation has an energetic cost which may be modeled as a function of the diameter. The curvature of the internal part of the cage decreases when m increases $[\mathcal{O}(1/m)]$, and this would favors cages of high diameters. As described in the text, this mechanism is in competition with the deformation of the termination [curvature of $\mathcal{O}(\sqrt{m})$].

As a first approximation, we can model the energy of NTSn cage of diameter m by the formula $E_{\mathrm{NTS}}(n,m)=(n-6)E_b(m)+2E_t(m)$. Here E_b is the energy of a slice in the internal part of the structure, and E_t is the energy associated with a deformed termination, which we assume in our picture to have the thickness of three slices. The values of E_b and E_t are found by considering the energies of two NTS cages with the same diameters and terminations. We took as references the NTS12 and NTS18 families, and also NTS24 for higher diameters.

The form of the functions E_b and E_t is obtained by expressing the energy of the cage surface within the isotropic shell model of elasticity theory, as has already been done for monolayers of materials with hexagonal symmetry in 2d lattices (see, e.g., Refs. 25 and 26). The local energy of a single slice of the body of a NTSn cage will then depend mainly of the square of its curvature, which implies $E_b(m)/m=A_b/m^2$. For the 2×1-like termination, the energetic contributions which does not take into account the curvature term should be taken into account. These terms are related to the reconstructions and the surface stretching and compression, which will be (for high values of m) independent of m. We found that a m dependence of the form $E_t(m)/m-A_b/m^2=C_t'/m+B_t'$ correctly fits the points. For the polygonal termination, the energy behavior will be dominated by the square of the curvature of the termination (thus a term which is linear in m) plus the effects from stretching and compression, which we model the same way: in that case $E_t(m)/m=A_tm+C_t/m+B_t$. We found the interpolating parameters to be, in meV: $A_b=3975$, $A_t=187$, $B_t=322$ $C_t=4801$, $B_t'=992$, $C_t'=4037$.

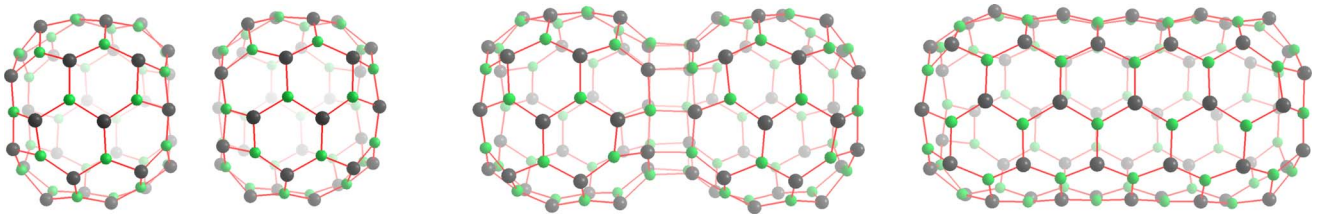

FIG. 6. (Color online) Fusion procedure of two NTS6 cages into one bigger NTS12 cage. As a first stage, it is energetically convenient to maximize the Si-C bonds. Eventually, the reduction of the deformation in the middle of the structure will complete the procedure.

In agreement with the DFT calculations, the above model also predicts that two cages NTSn_1 and NTSn_2 would always have the tendency to "fuse" in one longer NTS(n_1+n_2) cage, with a energy gain which only depends of the diameter, since $\forall m\ E_{\mathrm{NTS}}(n_1,m)+E_{\mathrm{NTS}}(n_2,m)-E_{\mathrm{NTS}}(n_1+n_2,m)=E_{\mathrm{NTS}}(0,m)>0$. The fusion procedure is sketched in Fig. 6 where we have drawn the pathway from two NTS6 cages of diameter $m=5$ (left panel) to one single NTS12 cage (right panel). The reaction occurs via an intermediate structure corresponding to two welded NTS6 (middle panel). For this diameter, the welding reaction as well as the transformation of the two welded NTSn into one NTS2n occurs spontaneously. As for the cutting, the first step of the reaction (the welding) is driven by the SiC bondings while the second part of the reaction is driven by the reduction of the deformation. It is worth noticing that the reactivity of the welding will be strongly affected by the alignment of the two NTSn.

The same kind of considerations can be applied to the 4–6 family. The average local structure of these cages is close to the undeformed SiC sheet, and it is altered by the presence of the six squares. The curvature induced by the squares forces the structures to have spheroidal shape. We may then argue that the main contribution to the energy of these structures comes from the spheroidal curvature, by the relation $E_{4\text{–}6}=A/d_{\mathrm{eff}}^2$, where $d_{\mathrm{eff}}=\sqrt{N_c}+\delta$. The a sphericity parameter δ takes into account the deviation of the cage from the pure spherical form. We fit the parameters $A=40.663$ eV, $\delta=2.45$, in good agreement with our results (see Fig. 4).

*pascal.pochet@cea.fr
†luigi.genovese@esrf.fr

[1] P. Mélinon, B. Masenelli, F. Tournus, and A. Perez, Nature Mater. **6**, 479 (2007).
[2] X.-H. Sun, C.-P. Li, W.-K. Wong, N.-B. Wong, C.-S. Lee, S.-T. Lee, and B.-K. Teo, J. Am. Chem. Soc. **124**, 14464 (2002).
[3] C. Ray, M. Pellarin, J. L. Lermé, J. L. Vialle, M. Broyer, X. Blase, P. Mélinon, P. Kéghélian, and A. Perez, Phys. Rev. Lett. **80**, 5365 (1998).
[4] L. Genovese, A. Neelov, S. Goedecker, T. Deutsch, S. A. Ghasemi, A. Willand, D. Caliste, O. Zilberberg, M. Rayson, A. Bergman, and R. Schneider, J. Chem. Phys. **129**, 014109 (2008).
[5] J. P. Perdew, K. Burke, and M. Ernzerhof, Phys. Rev. Lett. **77**, 3865 (1996).
[6] C. Hartwigsen, S. Goedecker, and J. Hutter, Phys. Rev. B **58**, 3641 (1998).
[7] M. Krack, Theor. Chem. Acc. **114**, 145 (2005).
[8] L. Genovese, T. Deutsch, A. Neelov, S. Goedecker, and G. Beylkin, J. Chem. Phys. **125**, 074105 (2006).
[9] L. Genovese, T. Deutsch, and S. Goedecker, J. Chem. Phys. **127**, 054704 (2007).
[10] M. Matsubara and C. Massobrio, J. Phys. Chem. A **109**, 4415 (2005).
[11] A. Srinivasan, M. N. Huda, and A. K. Ray, Eur. Phys. J. D **39**, 227 (2006).
[12] M. Huda and A. Ray, Chem. Phys. Lett. **457**, 124 (2008).
[13] M. Matsubara, J. Kortus, J.-C. Parlebas, and C. Massobrio, Phys. Rev. Lett. **96**, 155502 (2006).
[14] A. Mavrandonakis, G. E. Froudakis, M. Schnell, and M. Mühlhäuser, Nano Lett. **3**, 1481 (2003).
[15] M. Menon, E. Richter, A. Mavrandonakis, G. Roudakis, and A. N. Andriotis, Phys. Rev. B **69**, 115322 (2004).
[16] K. M. Alam and A. K. Ray, Phys. Rev. B **77**, 035436 (2008).
[17] R. Wang, D. Zhanga, and C. Liu, Chem. Phys. Lett. **411**, 333 (2005).
[18] M.-L. Sun, Z. Slanina, and S.-L. Lee, Chem. Phys. Lett. **233**, 279 (1995).
[19] R. Tenne, Nat. Nanotechnol. **1**, 103 (2006).
[20] H.-S. Wu, F.-Q. Zhang, X.-H. Xu, C.-J. Zhang, and H. Jiao, J. Phys. Chem. A **107**, 204 (2003).
[21] R. R. Zope, EPL **85**, 68005 (2009).
[22] R. Zope and B. I. Dunlap, Chem. Phys. Lett. **386**, 403 (2004).
[23] J.-Ch. Charlier, X. Blase, A. De Vita, and R. Car, Appl. Phys. A: Mater. Sci. Process. **68**, 267 (1999).
[24] S. Hou, J. Zhang, Z. Shen, X. Zhao, and Z. Xue, Physica E **27**, 45 (2005).
[25] M. Zhao, Y. Xia, F. Li, R. Q. Zhang, and S.-T. Lee, Phys. Rev. B **71**, 085312 (2005).
[26] K. N. Kudin, G. E. Scuseria, and B. I. Yakobson, Phys. Rev. B **64**, 235406 (2001).
[27] S. R. Lustig, E. D. Boyes, R. H. French, T. D. Gierke, M. A. Harmer, P. B. Hietpas, A. Jagota, R. S. McLean, G. P. Mitchell, G. B. Onoa, and K. D. Sams, Nano Lett. **3**, 1007 (2003).